GUT MICROBES
2020, VOL. 11, NO. 4, 997–1014
https://doi.org/10.1080/19490976.2020.1734423

Taylor & Francis
Taylor & Francis Group

RESEARCH PAPER

Lactobacillus reuteri maintains intestinal epithelial regeneration and repairs damaged intestinal mucosa

Haiqin Wu*, Shuang Xie*, Jinfeng Miao*, Yuchen Li, Zhihua Wang, Minjuan Wang, and Qinghua Yu

MOE Joint International Research Laboratory of Animal Health and Food Safety, College of Veterinary Medicine, Nanjing Agricultural University, Nanjing, Jiangsu, PR China

ABSTRACT

Little is known about the regulatory effect of microbiota on the proliferation and regeneration of ISCs. Here, we found that *L. reuteri* stimulated the proliferation of intestinal epithelia by increasing the expression of R-spondins and thus activating the Wnt/β-catenin pathway. The proliferation-stimulating effect of *Lactobacillus* on repair is further enhanced under TNF -induced intestinal mucosal damage, and the number of $Lgr5^+$ cells is maintained. Moreover, compared to the effects of *C. rodentium* on the induction of intestinal inflammation and crypt hyperplasia in mice, *L. reuteri* protected the intestinal mucosal barrier integrity by moderately modulating the Wnt/β-catenin signaling pathway to avoid overactivation. *L. reuteri* had the ability to maintain the number of $Lgr5^+$ cells and stimulate intestinal epithelial proliferation to repair epithelial damage and reduce proinflammatory cytokine secretion in the intestine and the LPS concentration in serum. Moreover, activation of the Wnt/β-catenin pathway also induced differentiation toward Paneth cells and increased antimicrobial peptide expression to inhibit *C. rodentium* colonization. The protective effect of *Lactobacillus* against *C. rodentium* infection disappeared upon application of the Wnt antagonist Wnt-C59 in both mice and intestinal organoids. This study demonstrates that *Lactobacillus* is effective at maintaining intestinal epithelial regeneration and homeostasis as well as at repairing intestinal damage after pathological injury and is thus a promising alternative therapeutic method for intestinal inflammation.

ARTICLE HISTORY
Received 24 June 2019
Revised 9 February 2020
Accepted 13 February 2020

KEYWORDS
Lactobacillus; intestinal epithelia; intestinal stem cells; proliferation; Wnt/β-catenin pathway

Introduction

The intestinal barrier is continuously exposed to intestinal microbiota and plays an important role in the homeostasis of mucosal function, which is maintained by efficient defensive reactions against chemical and microbial challenges.[1,2] An essential function of the intestinal mucosa is to act as a barrier between luminal contents and the underlying immune system.[3] Recent studies have demonstrated that the intestinal microbiota plays a very important role in health by benefiting the immune system and maintaining the intestinal barrier and many other aspects of health.[2,4] However, infectious intestinal pathogens, including various bacteria and viruses, have different mechanisms to damage the intestinal mucosal barrier and induce intestinal inflammation-related disorders, such as inflammatory bowel disease (IBD).[5] Although the causes of IBD are still unclear, increasing evidence has demonstrated that intestinal microbiota dysfunction is closely related to intestinal inflammation.[6,7]

The intestinal epithelium is replaced every 2–3 days in mice and every 3–5 days in humans, and the process is driven by continuous proliferation of intestinal stem cells (ISCs) that reside at the base of the crypt.[8,9] The delicate balance in ISCs between self-renewal and differentiation controls epithelial homeostasis and regeneration, particularly in response to mucosal injury and inflammation.[10] The activity of ISCs is tightly regulated by several niche-signaling pathways to balance intestinal homeostasis under physiological and pathological stimulation.[11,12] Among the modulators of ISCs in crypt niches, the Wnt/β-catenin signaling pathway is indispensable for stem cell expansion and crypt formation, which is highest at the crypt base, and transit-amplifying (TA) cells undergo proliferation.[13-16] Recent studies have already demonstrated that Paneth cells and

CONTACT Qinghua Yu yuqinghua1981@njau.edu.cn MOE Joint International Research Laboratory of Animal Health and Food Safety, College of Veterinary Medicine, Nanjing Agricultural University, Weigang 1, Nanjing, Jiangsu 210095, PR China
*These authors contributed equally to this work.
Supplemental data for this article can be accessed on the publisher's website

subepithelial myofibroblasts secrete epidermal growth factor, transforming growth factor (TGF), and Wnt3 for the maintenance of ISCs, whereas their maturation depends on Wnt signaling.[17,18] Although the intestinal microbiota closely contacts intestinal epithelia, the detailed mechanism by which the intestinal microbiota affects ISC niches remains unknown.

Lactobacillus spp. is an important probiotic and is extensively used in dairy food, which helps hosts with nutritional assistance, immune system maturation, protection of mucosal barrier function and prevention of injurious effects caused by xenobiotics and pathogens.[19,20] However, recent studies on the benefits of *Lactobacillus* to gut health have mainly focused on its modulation of tight junctions, immune response or reduction in pH values. Recent studies indicated that *Lactobacillus* stimulates reactive oxygen species (ROS) production *via* the nicotinamide adenine dinucleotide phosphate (NADPH) oxidase family of enzymes (Nox) to activate ISC proliferation under physiological conditions.[21] Our previous study demonstrated that the *L. reuteri* metabolite indole-3-aldehyde stimulated lamina propria lymphocytes (LPLs) to secrete interleukin-22 (IL-22) through aryl hydrocarbon receptor (AhR) and then induced phosphorylation of signal transducer and activator of transcription 3 (STAT3) to accelerate the proliferation of intestinal epithelia, thus ameliorating damaged intestinal mucosa.[22] However, we are still not clear whether *L. reuteri* could modulate the Wnt/β-catenin signaling pathway to stimulate the proliferation of ISCs.

Previous studies exploring the interaction between intestinal microbiota and intestinal epithelia have always used intestinal epithelial cell lines, such as Caco-2 cells, which do not completely mimic the real situation in the gut. Intestinal organoids, containing ISCs, can proliferate and differentiate into all intestinal epithelial cell lines, such as absorptive, goblet, Paneth and tuft cells.[23–25] Understanding intestinal organoids, which could develop into intestinal villi and crypts, is a breakthrough for studying the crosstalk between intestinal mucosa and intestinal microbiota.[26,27] In this study, we explored the stimulatory effect of *L. reuteri* on the proliferation of ISCs under physiological and pathological conditions. Moreover, we also detected the protective effects of *L. reuteri* against *C. rodentium*-induced intestinal inflammation.

Results

L. *reuteri* increased the proliferation of intestinal organoids under physiological conditions

To assess the stimulatory effect of *L. reuteri* D8 on intestinal epithelia, we successfully isolated crypts from the small intestines of mice and cultured them in Matrigel as indicated in the schematic diagram (Figure 1(a)). The organoids began to bud on the third day (Figure 1(b)), at which point they were passaged and cultured for 1 day and then treated with D8 (10^6 CFU) for 48 h. The surface area of intestinal organoids increased significantly under *L. reuteri* D8 treatment (Figure 1(c)). *L. reuteri* stimulated intestinal epithelial proliferation with significantly increased mRNA expression of c-Myc, cyclin and Ki67 (Figure 1(d)), which was also verified with significantly enhanced proliferating cells stained with 5-ethynyl-2′-deoxyuridine (EdU) in crypts (Figure 1(e)).

Activation of the Wnt/β-catenin pathway by L. *reuteri* promoted intestinal epithelial proliferation

Wnt/β-catenin signals are essential for intestinal epithelium homeostasis, while the Wnt-LRP5/6 complex transduces a signal into the cell, resulting in nuclear accumulation of β-catenin and subsequent activation of T cell factor (TCF) target genes.[28] *L. reuteri* D8 activated the Wnt/β-catenin pathway by significantly increasing the mRNA expression levels of Wnt3 and Lrp5 (Figure 2(a)), which was also further verified by increased β-catenin and active β-catenin expression (Figure 2(b)). As expected, *L. reuteri* D8 induced obvious nuclear accumulation of active β-catenin, which was similar to the results of a Wnt agonist 1 application (Figure 2(c)). The mRNA expression levels of ISC marker genes, such as active ISC markers (Lgr5, Olfm4, Ascl2) and quiescent ISC markers (Bmi1, Msi1), were also increased in organoids cocultured with *L. reuteri* D8 (Figure 2(d)). Moreover, compared to those in the control group, the Lgr5 protein levels and $Lgr5^+$ cell numbers were increased in organoids treated with *L. reuteri* (Figure 2(e,f)).

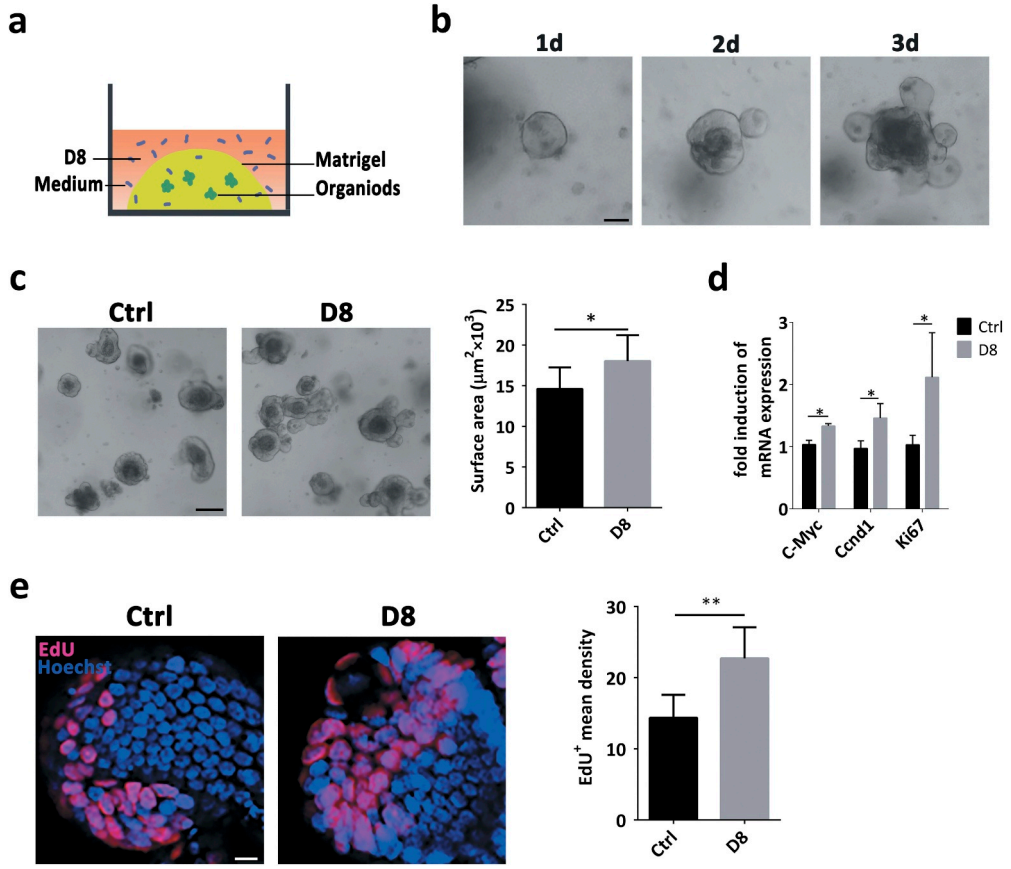

Figure 1. *L. reuteri* D8 upregulated intestinal organoid proliferation under physiological conditions. (a) Coculture model of *L. reuteri* D8 and organoids. (b) Crypts from small intestines were seeded onto Matrigel and cultured for 3 days to obtain well-developed organoids. Scale bars, 100 μm. (c) Organoids were treated with or without *L. reuteri* D8 (10^6 CFU per well) for 48 h. The surface area of organoids was calculated. Scale bars, 50 μm; $n = 6$. (d) RT-qPCR analysis of the fold induction of the proliferation genes c-Myc, cyclin and Ki67 in organoids treated with/without D8; $n = 6$. (e) Confocal images of organoid staining with Hoechst (blue) and EdU (red); scale bar, 10 μm. The mean density of EdU-positive cells in each organoid was calculated. $n = 6$. Data are presented as the mean ± SD. $^*P < .05$, $^{**}P < .01$. Data were combined from at least three independent experiments unless otherwise stated.

The R-Spondin proteins are implicated in the activation of the Wnt signaling pathway, even in the absence of leucine-rich repeat-containing G-protein coupled receptors (LGRs).[29,30] We also found that without R-spondins in the culture medium, the mRNA expression of Wnt/β-catenin pathway genes (Wnt3, Lgr5 and c-Myc) was significantly reduced (Figure 2(g)). Interestingly, *L. reuteri* D8 could still increase the mRNA expression of Wnt3, Lgr5 and c-Myc even in the absence of R-spondins (Figure 2(g)). We also found that *L. reuteri* D8 could increase the mRNA expression of R-spondin-1, R-spondin-2 and R-spondin-3 (Figure 2(h)). This phenomenon was also verified with increased EdU^+ cell numbers in organoids. Moreover, the stimulatory effect of live *L. reuteri* on proliferation was more obvious than that of heat-killed *Lactobacillus* (Figure 2(i)).

L. reuteri alleviated TNF -induced intestinal epithelial damage

In addition to assessing the stimulatory effect of *L. reuteri* D8 under physiological conditions, we also determined whether *L. reuteri* D8 possesses an intestinal epithelial repair function in pathological states, such as intestinal inflammation caused by TNF in intestinal organoids.[31] Obvious damage to intestinal organoids was observed after TNF treatment, and more than 80% of organoids were disrupted within 36 h (Figure 3(a)). However, *L. reuteri* D8 significantly reduced the percentage of disrupted organoids and TNF expression, which was consistent with the reduced apoptotic cells (Figure 3(b,c)).

EdU is incorporated into the DNA of dividing cells, and EdU staining thus provides a sensitive

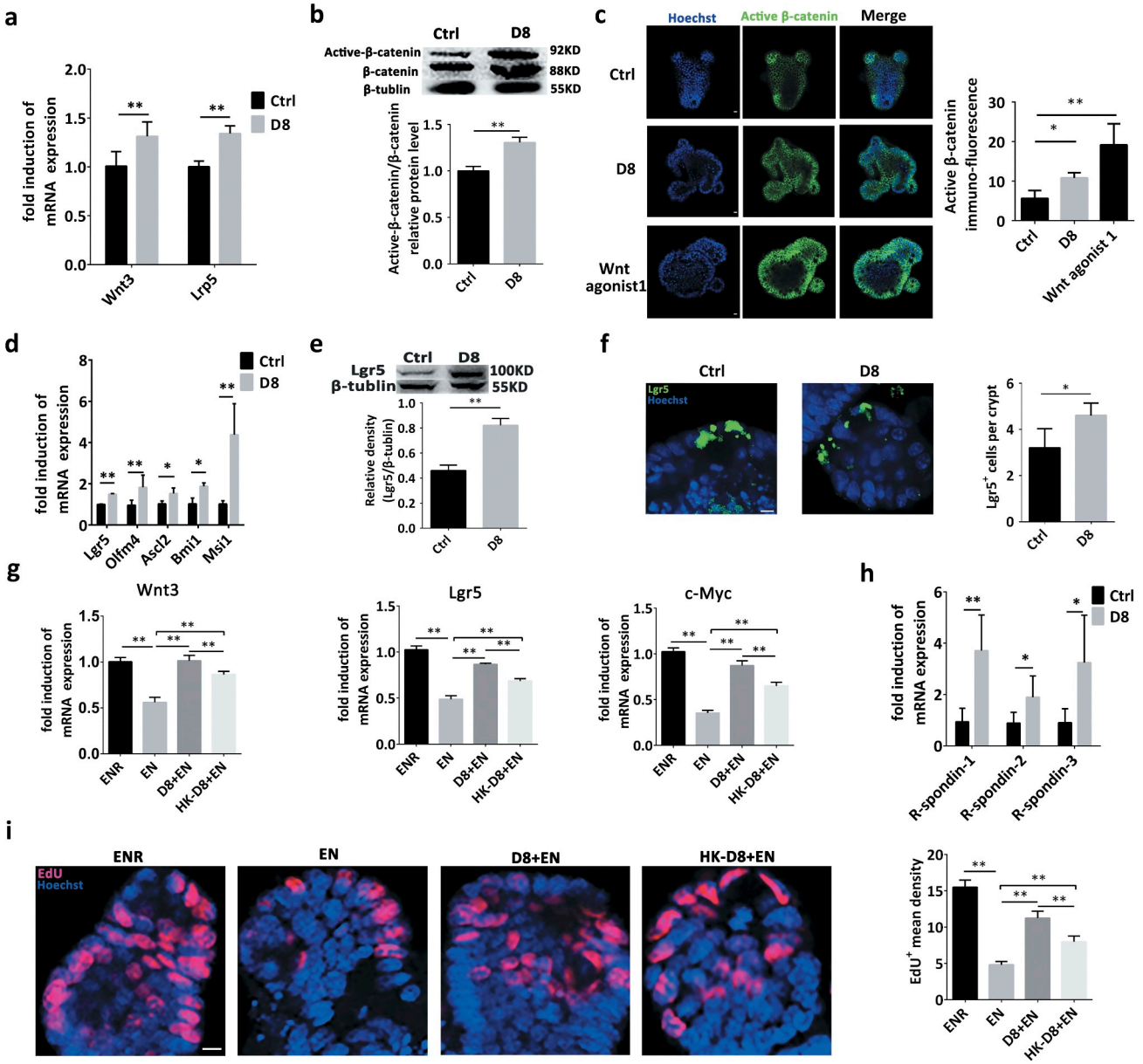

Figure 2. *L. reuteri* activated the Wnt/β-catenin pathway and promoted ISC proliferation. (a) Organoids were treated with or without *L. reuteri* D8 (10^6 CFU per well) for 48 h respectively. RT-qPCR analysis of the fold induction of Wnt3 and Lrp5 expression in organoids cultured with or without D8 (10^6 CFU); $n = 6$. (b) Western blot analysis of active β-catenin and β-catenin expression in organoids; $n = 6$. (c) Organoids were co-cultured with *L. reuteri* D8 (10^6 CFU) or Wnt agonist 1(10 μM) for 24 h respectively. Confocal images of organoid staining with Hoechst (blue) and active β-catenin (green). The average fluorescence intensity of active β-catenin was analyzed by Image-Pro Plus, $n = 6$. (d) Fold induction of active ISC markers (Lgr5, Ascl2, Olfm4) and quiescent ISC markers (Bmi1, Msi1) in organoids; $n = 6$. (e) Western blot results of Lgr5 protein expression in organoids; $n = 6$. (f) Confocal images of organoid staining with Hoechst (blue) and Lgr5 (green). The Lgr5-positive cells in each crypt were detected. $N = 6$. (g) The Wnt3, Lrp5 and c-Myc mRNA expression in different groups was detected by RT-qPCR, $n = 6$. ENR = EGF+Noggin+R-spondin, EN = EGF+Noggin. (h) r-spondin-1, r-spondin-2 and r-spondin-3 mRNA expression in organoids was detected by RT-qPCR; $n = 6$. (i), Organoids were stained with EdU (red). Nuclei were stained with Hoechst (blue); *c*. Data are presented as the mean ± SD. $^*P < .05$, $^{**}P < .01$. Data were combined from at least three independent experiments unless otherwise stated.

and robust method to detect and quantify intestinal epithelium proliferation.[32] In this study, *L. reuteri* also ameliorated the loss of EdU^+ cells caused by TNF treatment to maintain the proliferative ability to repair the damaged epithelia (Figure 3(d)). Furthermore, *L. reuteri* reversed the reduced expression of c-Myc, cyclin and Ki67 after TNF treatment (Figure 3(e)). Compared to that of *L. reuteri* D8, the ability of *L. salivarius* C5 to accelerate intestinal epithelial proliferation, as

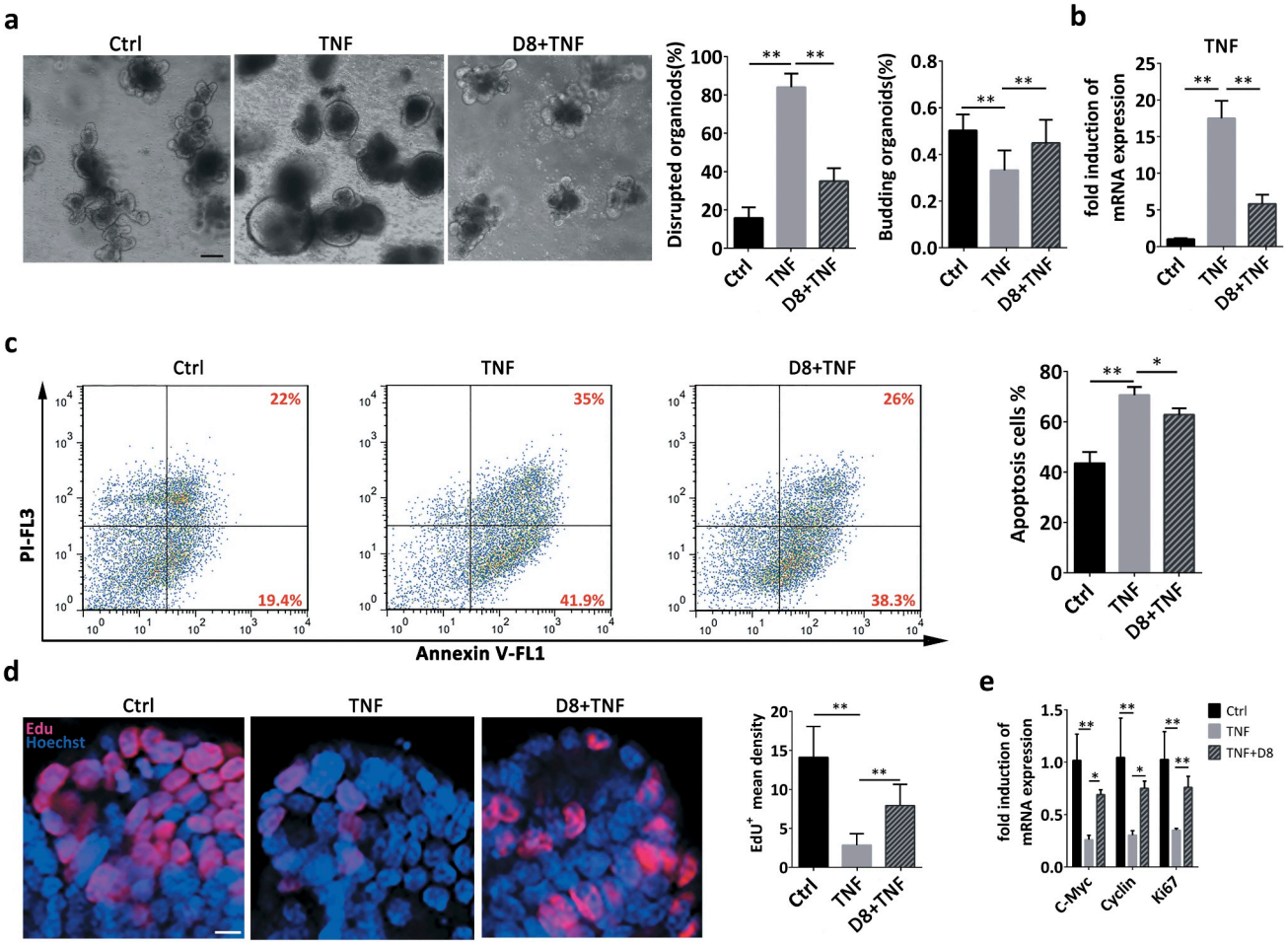

Figure 3. The inflammatory response induced by TNF was reduced by *L. reuteri*. (a) Organoids were treated with TNF (60 ng/mL) for 12 h alone or cocultured with *L. reuteri* (10^6 CFU) for another 36 h. Organoid morphology was assessed by light microscopy; $n = 6$. The number of damaged organoids per well was counted; $n = 6$. Scale bars, 100 μm. (b) TNF mRNA expression in organoids was detected by RT-qPCR; $n = 6$. (c) Annexin V-PI double staining was performed to distinguish early apoptotic cells (Annexin V^+, PI^-) from late apoptotic cells (Annexin V^+, PI^+); $n = 6$. (d) Confocal images of nuclear staining (blue) and EdU staining (red) in organoids. $n = 6$. Scale bar, 100 μm. (e) RT-qPCR analysis of the fold induction of the proliferation genes c-Myc, cyclin, Ki67 in organoids; $n = 6$. Data are presented as the mean ± SD. $^*P < .05$, $^{**}P < .01$. Data were combined from at least three independent experiments unless otherwise stated.

measured by the mRNA expression of c-Myc, Lgr5 and EdU staining, was weaker in the pathological state (Sup. Fig. 1A, 1B and 1 C).

L. reuteri D8 maintained activation of the Wnt/β-catenin pathway to repair TNF -induced damage to intestinal epithelia

To explore the modulatory effect of *L. reuteri* on the Wnt/β-catenin pathway, intestinal organoids were treated with *L. reuteri*. Compared to the TNF-alone treated group, *L. reuteri* D8 significantly upregulated Wnt3 and Lrp5 expression, which was consistent with the enhanced protein expression of β-catenin (Figure 4(a,b)). Interestingly, TNF inhibited the mRNA expression of the active stem cell markers Lgr5, Olfm4, and Ascl2 and increased the expression of the quiescent stem cell marker Msi1. Moreover, *L. reuteri* significantly increased Lgr5, Olfm4, Ascl2 and Bmi1 expression (Figure 4(c)). The maintenance of ISCs was also further verified by the increased protein expression of Lgr5 and $Lgr5^+$ cell numbers in crypts (Figure 4 (d,e)). These results demonstrated that *L. reuteri* maintained the activation of the Wnt/β-catenin pathway inhibited by TNF and thus stimulated the proliferation of intestinal epithelia. Lysozyme is always used as a Paneth cell marker,[33,34] and TNF significantly decreased the number of Paneth cells in the crypt and lysozyme expression compared to those in the control group, indicating Paneth cell dysfunction

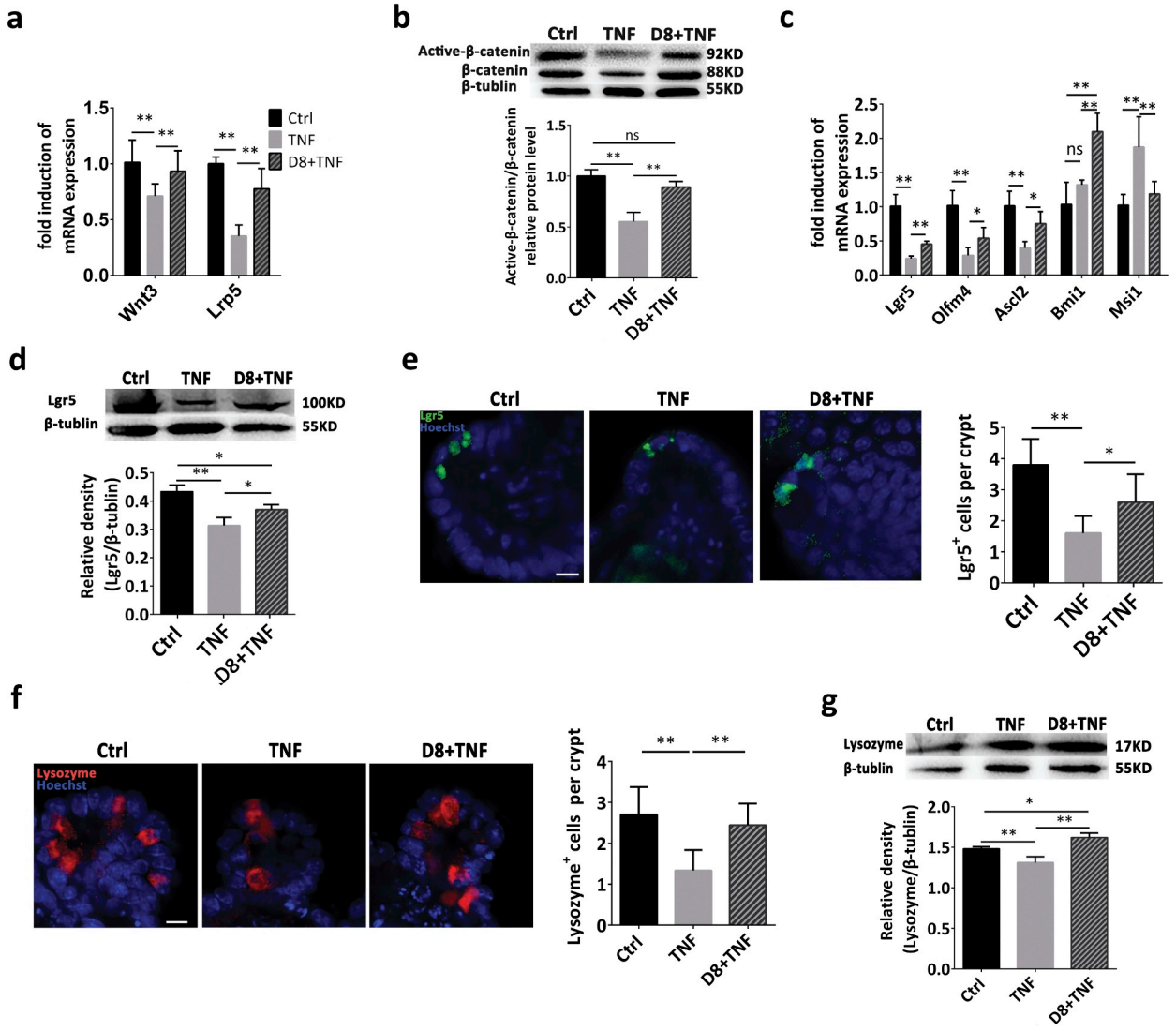

Figure 4. *L. reuteri* enhanced ISC regeneration via moderately activating the Wnt/β-catenin pathway. Organoids were treated with TNF (60 ng/mL) for 12 h alone or cocultured with *L. reuteri* (10^6 CFU) for another 36 h. (a) RT-qPCR analysis of the fold induction of Wnt3 and Lrp5 expression in organoids; $n = 6$. (b) Western blot analysis of β-catenin and active β-catenin expression in organoids; $n = 6$. (c) Fold induction of Lgr5, Olfm4, Ascl2, Bmi1 and Msi1; $n = 6$. (d) Western blot and densitometry analysis of Lgr5 expression; $n = 6$. (e) Confocal images of Lgr5 staining (green) and Hoechst staining (blue) in organoids. The number of $Lgr5^+$ cells in each crypt was counted; $n = 6$. Scale bar, 100 μm. (f) Organoids were stained with lysozyme (red) and Hoechst (blue); $n = 6$; the number of $lysozyme^+$ cells per crypt was calculated. (g) Western blot and densitometry analysis of lysozyme expression in organoids; $n = 6$. Data are presented as the mean ± SD. $^*P < .05$, $^{**}P < .01$. Data were combined from at least three independent experiments unless otherwise stated.

(Figure 4(f,g)). However, *L. reuteri* D8 restored the number of Paneth cells and lysozyme expression after organoid damage induced by TNF (Figure 4(f,g)).

L. reuteri protected the intestinal mucosal barrier against C. rodentium infection

First, to verify colonization of *L. reuteri* D8 in the intestine, mice were orally administered 10^8 CFU *L. reuteri* D8 suspended in 200 μL of PBS only once, colonization of *L. reuteri* reached peak (5.5×10^6 CFU) at 16 h and maintained at the level of 4.3×10^5 CFU 24 h post administration (Figure 5(a)), which was further confirmed with the observation of fluorescence labeled *L. reuteri* D8 by immunofluorescence microscopy at 16 h (Figure 5(b)). To further confirm the protective effect of *L. reuteri* D8 on ameliorating intestinal inflammation in vivo, C57BL/6 mice were orally administered *L. reuteri* D8 (Figure 5(c)). Moreover, the colonization of *L. reuteri*

significantly reduced the number of *C. rodentium* in feces (Figure 5(d)) and the weight loss (Figure 5(e)) induced by *C. rodentium* infection.

The intestine of *C. rodentium*-infected mice became bloated and transparent (Figure 5(f)). However, *L. reuteri* D8 greatly decelerated the pathological damage and maintained normal crypt depth to avoid crypt hyperplasia (Figure 5(g,h)). However, heat-killed *L. reuteri* showed a weaker protective effect against *C. rodentium* infection in regards to body weight, pathological changes and crypt hyperplasia (Figure 5(e–h)). The pathological changes in intestinal morphology caused by *C. rodentium* infection were consistent with the increased concentration of LPS in serum (Figure 5(i)) and the secretion of the proinflammatory cytokines TNF and IL-1β in the intestine (Figure 5(j)). Moreover, live *L. reuteri* exhibited a stronger effect on reducing LPS and proinflammatory cytokine levels than heat-killed *L. reuteri* (Figure 5(i,j)).

L. reuteri modulated ISC niches to affect ISC proliferation and differentiation

To uncover the protective effect of *L. reuteri* against *C. rodentium* infection, activation of the Wnt/β-catenin pathway and Paneth cell differentiation were explored. *C. rodentium* increased the mRNA expression of Wnt3, Lrp5 and Lgr5 to activate the Wnt/β-catenin pathway, which is inconsistent with the increased crypt depth and crypt hyperplasia. However, *L. reuteri* alleviated the activation level of the Wnt/β-catenin pathway to avoid overactivation (Figure 6(a)). This regulatory effect was further verified with moderate c-Myc expression induced by live *L. reuteri* D8 (Figure 6(b)). Moreover, *L. reuteri* also increased the density of proliferating cell nuclear antigen (PCNA)-positive cells to a moderate level to stimulate the proliferation of intestinal epithelia in response to the gentle activation of the Wnt/β-catenin pathway (Figure 6(c)). A similar regulatory effect of *L. reuteri* was also detected for the $Lgr5^+$ cells in crypts (Figure 6(d)). However, *C. rodentium* infection reduced the density of $lysozyme^+$ Paneth cells, while *L. reuteri* significantly influenced the differentiation of ISCs and reversed this phenomenon (Figure 6(e)). *L. reuteri* not only increased the density of $lysozyme^+$ Paneth cells but also increased the mRNA expression of antimicrobial peptide genes, such as Defa1, Defa6 and Lyz-1, to prevent *C. rodentium* infection (Figure 6(f)).

Confirmation of the protective effect of L. reuteri against C. rodentium infection in mice and intestinal organoids

To further confirm the protective effect of *L. reuteri* via activation of the Wnt/β-catenin pathway, the Wnt antagonist Wnt-C59 was orally administered to mice (Figure 7(a)). The protective effect of *L. reuteri* on alleviating body weight loss, *C. rodentium* colonization and pathological changes were reversed with the addition of the Wnt antagonist Wnt-C59 (Figure 7(b–d)). The proliferative ability, as determined by PCNA staining, and the mRNA expression of Wnt3 and Lgr5 were inhibited by the application of the Wnt antagonist Wnt-C59 (Figure 7(e,f)), which was consistent with the reduction in R-spondin-1 expression (Figure 7(g)). Moreover, Wnt-C59 also inhibited the differentiation of Paneth cells and their expression levels of antimicrobial peptides (Defa1, Defa6 and Lyz-1) (Figure 7(h–j)). These results could then explain the increased TNF and IL-1β expression and LPS concentration even with *L. reuteri* treatment (Figure 7(k,l)).

To exclude the complex function of intestinal microbiota, intestinal organoids were also treated with the Wnt antagonist Wnt-C59 to further confirm the modulatory effect of *L. reuteri* on the Wnt/β-catenin pathway and Paneth cells. With the addition of Wnt-C59 to the medium, *L. reuteri* could no longer protect intestinal organoids from *C. rodentium*-induced damage, and the number of *C. rodentium* colonies increased (Figure 8(a,b)). The modulatory effect of *L. reuteri* on the Wnt/β-catenin pathway was also reversed by Wnt-C59, with reduced expression of Wnt3, Lgr5 and R-spondin-1 (Figure 8(c,d)). Moreover, Wnt-C59 also inhibited the *L. reuteri*–induced differentiation of Paneth cells and antimicrobial peptide expression in organoids (Figure 8(e–g)), which is closely related to increased inflammatory cytokine expression (Figure 8(h)).

Discussion

The intestinal tract is continuously inflamed at low levels, which is necessary to stimulate immune

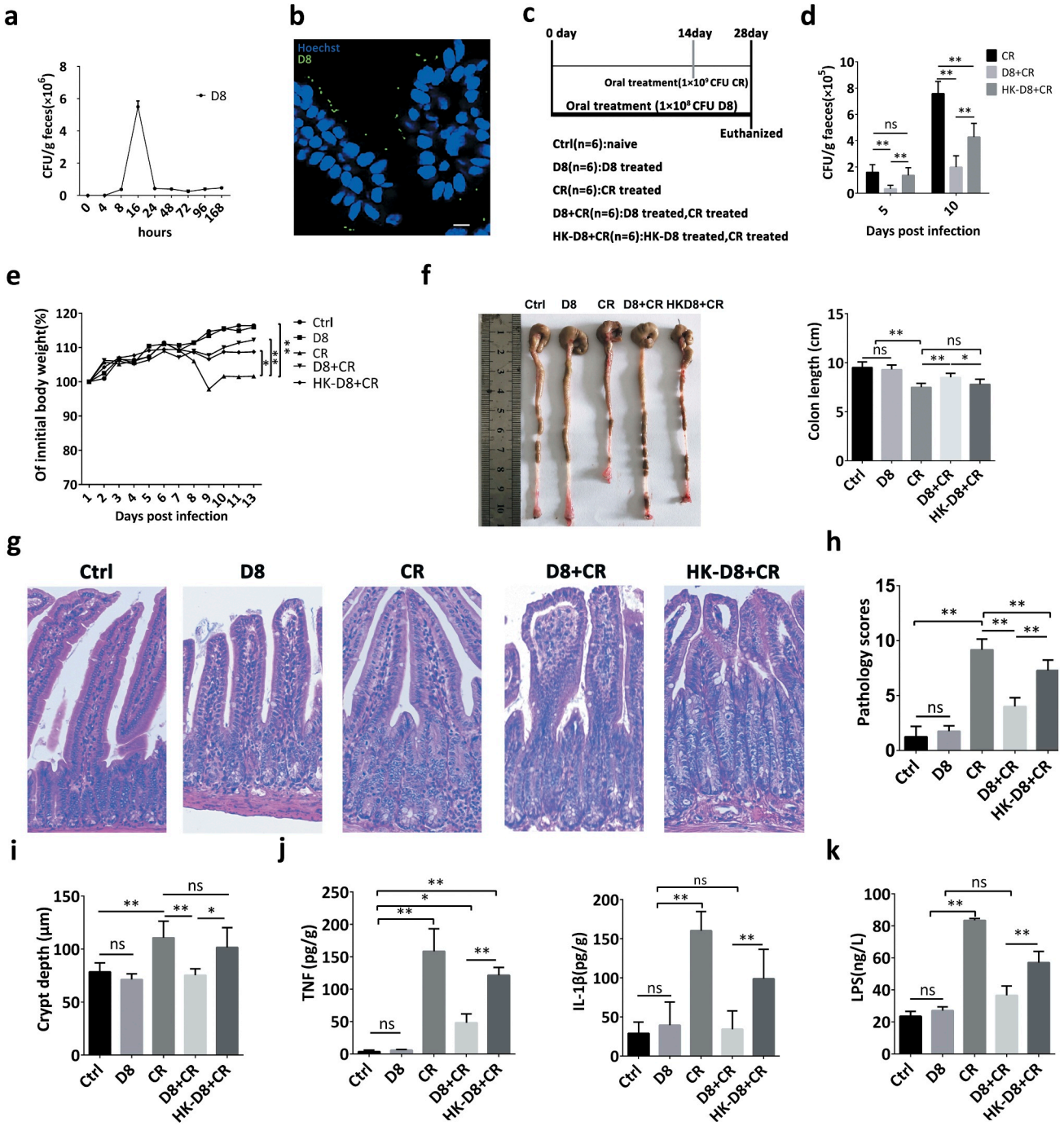

Figure 5. *L. reuteri* reduced *C. rodentium* colonization and ameliorated intestinal inflammation in mice. (a) To verify colonization of *L. reuteri* D8 in the intestine, mice were orally administered *L. reuteri* D8 (10^8 CFU) only once, and the number of *L. reuteri* D8 colonies in mouse feces on MRS plates containing tetracycline (500 μg/ml) was detected at the indicated time points. (b) *L. reuteri* D8 labeled with BacLight™ Bacterial Green Stain (10^8 CFU) was administered to mice, intestinal tissue was collected 16 h post administration, and the distribution of *L. reuteri* in the intestine was detected by confocal microscopy; D8 (green), Hoechst (blue). (c) A schematic of the animal treatment strategy. Four-week-old mice were orally administered 200 μl of *L. reuteri* (10^8 CFU), HK-*L. reuteri* (10^8 CFU) and PBS for 28 days continuously, and the infection groups were orally administered 200 μl of *C. rodentium* (10^9 CFU) on the 14th day. The mice were sacrificed after subjection to the different treatments on the 28th day. (d) The number of *C. rodentium* colonies in mouse feces was detected with MacConkey agar plates. (e) Mouse body weight changes during the course of the experiments. (f, g) Photomicrographs of mice and ileum pathology scores. Scale bars, 200 μm. (h) Segments of ileum were processed to measure the crypt depth. (i) The LPS concentration in serum samples was detected by ELISA; $n = 6$. (j) IL-β and TNF secretion in ileal tissue supernatant was detected by ELISA, $n = 6$. Data are presented as the mean ± SD. $^*P < .05$, $^{**}P < .01$. Data were combined from at least three independent experiments unless otherwise stated.

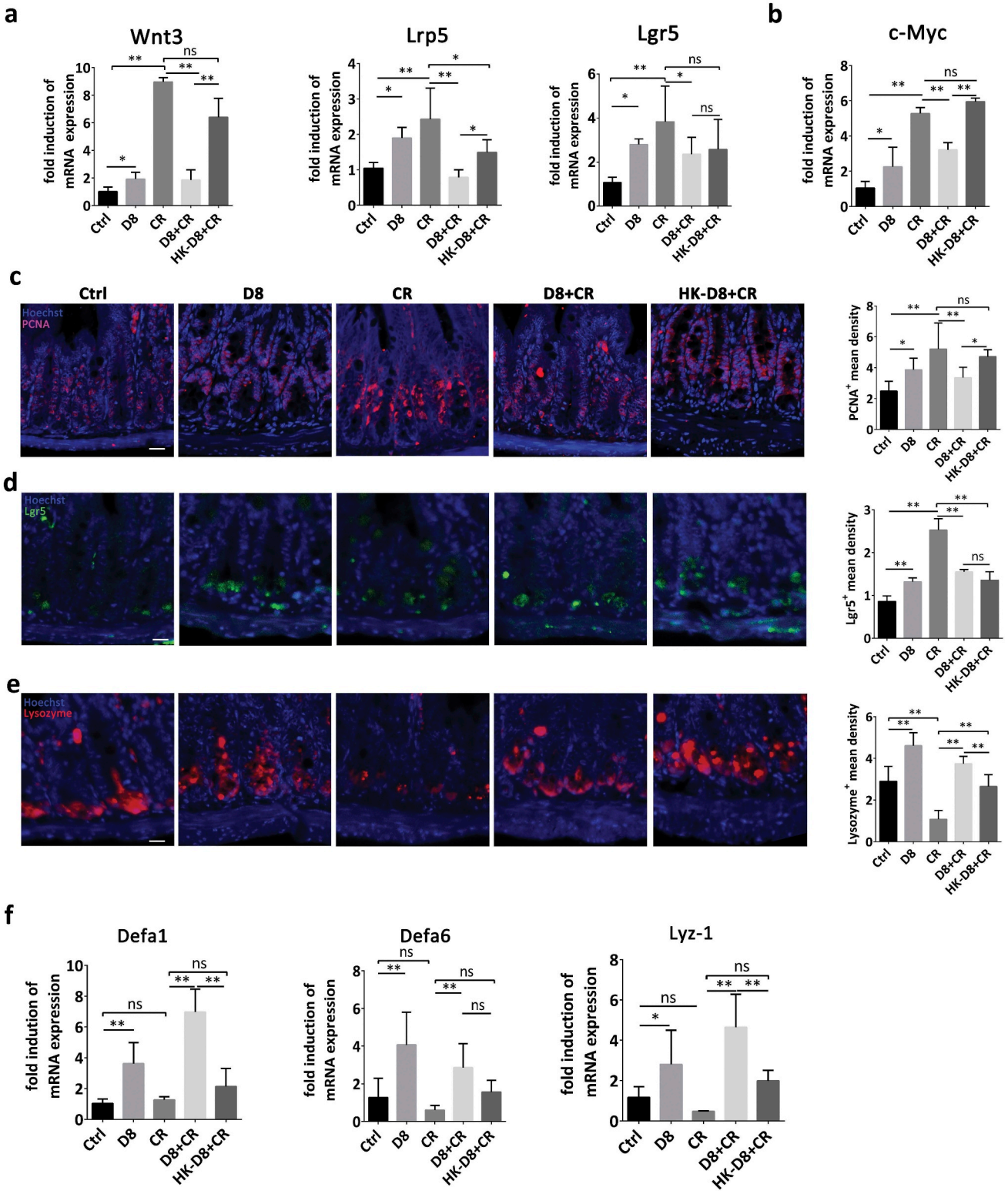

Figure 6. *L. reuteri* maintained normal levels of lgr5$^+$ ISCs and lysozyme$^+$ Paneth cells to moderately stimulate epithelial proliferation after *C. rodentium* infection. (a) RT-qPCR analysis of the fold induction of Wnt3, Lrp5 and Lgr5 expression; $n = 6$. (b) c-Myc mRNA expression was detected by RT-qPCR, $n = 6$. (c) Confocal images of ileal tissues stained with PCNA (red) and Hoechst (blue). The mean density of PCNA$^+$ cells per crypt was detected. Scale bars, 200 μm. (d) Confocal images (Lgr5 staining, green; Hoechst staining, blue) of ileum. The mean density of Lgr5-positive cells per crypt was detected. Scale bars, 200 μm. (e) Confocal images of lysozyme staining (red) and Hoechst staining (blue) in the ileum. The mean density of lysozyme+ cells per crypt was detected. (f) Fold induction of Defa1, Defa6, and lysozyme expression; $n = 6$. Data are presented as the mean ± SD. $^*P < .05$, $^{**}P < .01$. Data were combined from at least three independent experiments unless otherwise stated.

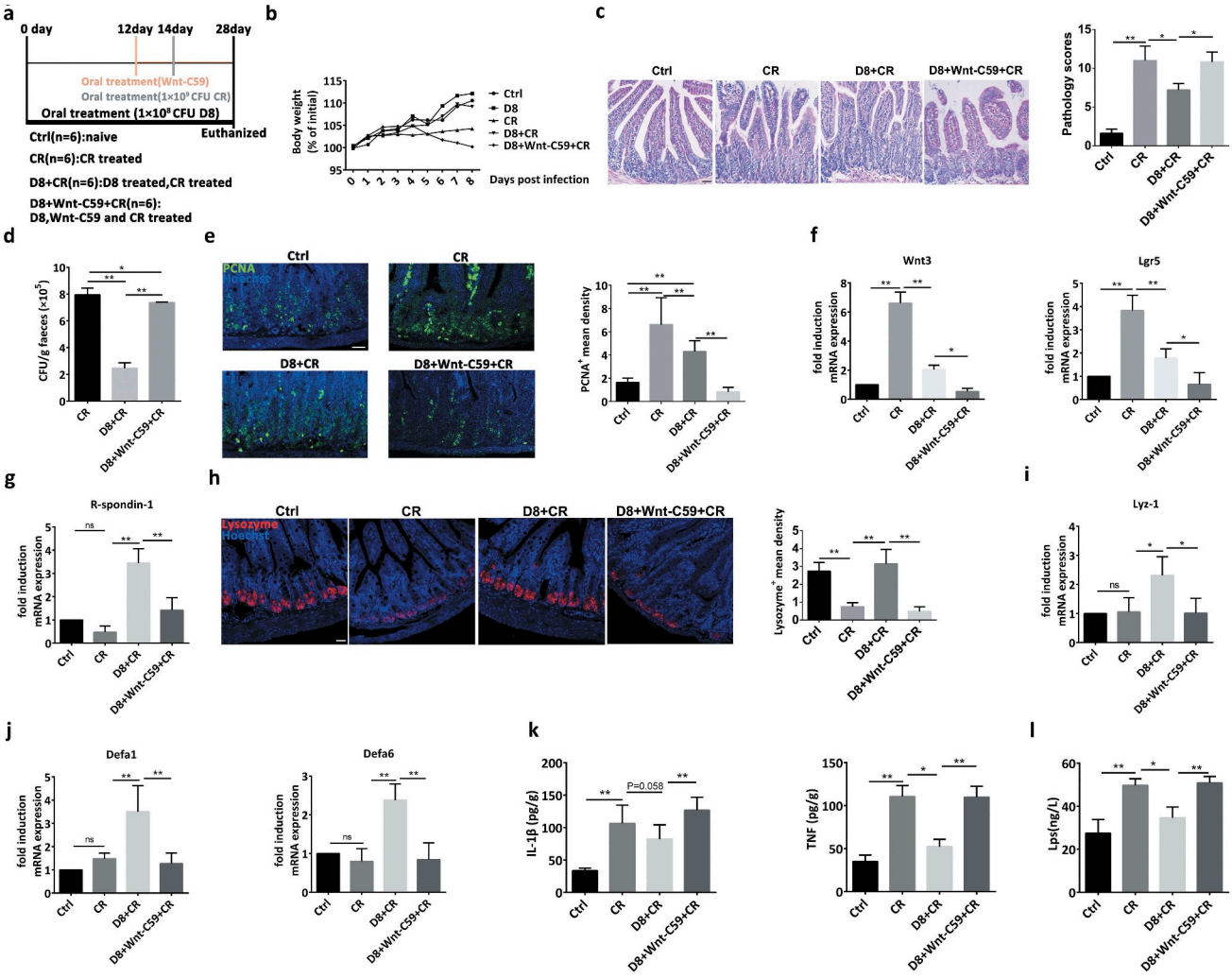

Figure 7. Confirmation of the protective effect of *L. reuteri* against *C. rodentium* infection in mice and intestinal organoid. (a) A schematic of the animal treatment strategy. The mice were sacrificed after subjection to the different treatments on the 28th day. (b) Mouse body weight changes during the course of the experiments. (c) Photomicrographs of mice and ileum pathology scores. Scale bars, 200 μm. (d) The number of *C. rodentium* colonies in mouse feces was detected with MacConkey agar plates. (e) Confocal images of ileal tissues stained with PCNA (green) and Hoechst (blue). The mean density of $PCNA^+$ cells per crypt was detected. Scale bars, 200 μm. (f–g) RT-qPCR analysis of the fold induction of Wnt3, Lgr5 and R-spondin1 expression; $n = 6$. (h) Confocal images of lysozyme staining (red) and Hoechst staining (blue) in the ileum. The mean density of lysozyme+ cells per crypt was detected. (i–j) RT-qPCR analysis of the fold induction of Lyz-1, Defa1 and Defa6 expression; $n = 6$. (k) IL-β and TNF secretion in ileal tissue supernatant was detected by ELISA, $n = 6$. (l) The LPS concentration in serum samples was detected by ELISA; $n = 6$. Data are presented as the mean ± SD. $^*P < .05$, $^{**}P < .01$. Data were combined from at least three independent experiments unless otherwise stated.

responses and ISC proliferation.[35,36] However, numerous factors, such as antibiotics, stress, food, and pathogen invasion, induce and exacerbate intestinal inflammation.[37] The intestinal microbiota plays a critical role in maintaining the intestinal mucosal barrier and resistance to pathogenic bacterial invasion.[38,39] However, due to the complexity of the intestinal microbiota, its relationship with epithelia is still unknown. In contrast to traditional intestinal epithelial cells, intestinal organoids containing ISCs represent a breakthrough for studying the interaction between microbiota and the intestinal mucosal barrier.[40] TNF is a key regulator of immunity and an important mediator of autoimmune diseases, such as arthritis and IBD.[41] The TNF model is useful to study acute inflammation states, such as sepsis, necrotizing enterocolitis, and intestinal hypoxia.[42,43] In this study, we explored the function of *Lactobacillus* in intestinal epithelia in the physiological state and the repair process after injury in an intestinal organoid

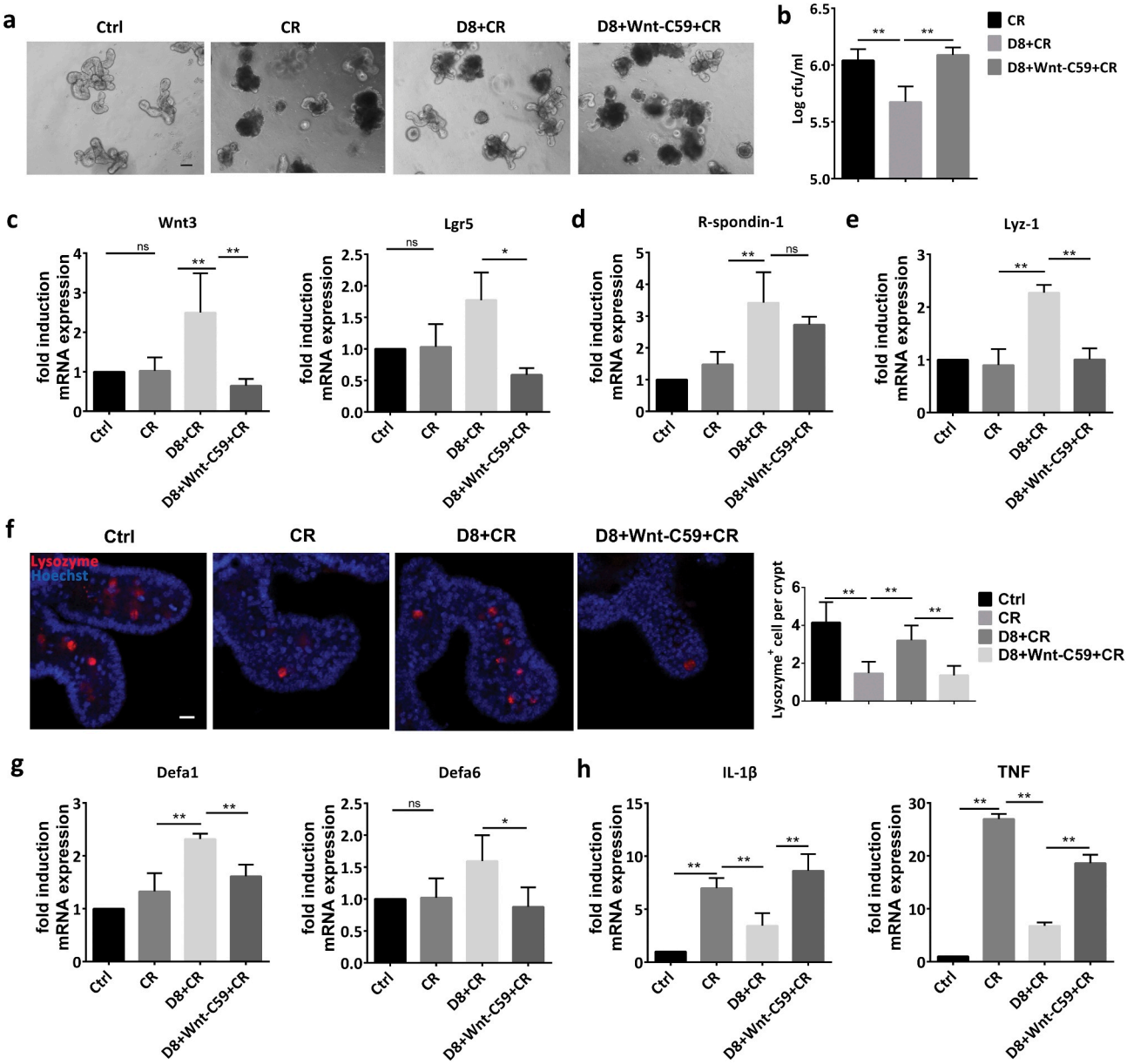

Figure 8. Confirmation of the protective effect of *L. reuteri* against *C. rodentium* infection in mice and intestinal organoids. (a) Organoids were treated with *C. rodentium* (10^6 CFU) alone or cocultured with *L. reuteri* (10^6 CFU) and Wnt-C59 (100 nM). Organoid morphology was assessed by light microscopy; $n = 6$. Scale bars, 100 μm. (b) The number of *C. rodentium* colonies per well was detected with MacConkey agar plates. (c–e) RT-qPCR analysis of the fold induction of Wnt3, Lgr5, R-spondin1 and Lyz-1 expression; $n = 6$. (f) Organoids were stained with lysozyme (red) and Hoechst (blue); $n = 6$; the number of lysozyme$^+$ cells per crypt was calculated. (g–h) RT-qPCR analysis of the fold induction of Defa1, Defa6, IL-1β and TNF expression; $n = 6$. Data are presented as the mean ± SD. $^*P < .05$, $^{**}P < .01$. Data were combined from at least three independent experiments unless otherwise stated.

model and mice. We found that under physiological conditions, intestinal organoids grew well when cocultured with *L. reuteri* D8, and obvious stimulatory effects were observed on the organoid surfaces under a light microscope. Moreover, *L. reuteri* reduced the morphological damage and the apoptosis ratio of intestinal organoids after TNF treatment, which may have been attributed to the reduced secretion of TNF. The increased number of EdU$^+$ cells and mRNA expression levels of c-Myc, cyclin and Ki67 in organoids indicated that *L. reuteri* D8 stimulated the proliferation of intestinal epithelia under physiological conditions and repaired the damaged epithelia under pathological conditions.

The Wnt/β-catenin pathway is crucial for the maintenance of intestinal crypt proliferation.[28,44,45]

Wnt ligands bind Frizzled and Lrp5/6 receptor complexes to induce the nuclear translocation of β-catenin via suppressing the Apc/Gsk-3β/Axin2 complex, leading to Tcf4/β-catenin complex formation.[46,47] Our previous study demonstrated that *L. reuteri* stimulated LPLs to secrete IL-22 and thus induced the activation of STAT3 to accelerate the proliferation of intestinal epithelia.[22] In this study, we further found that *L. reuteri* also had the ability to activate the Wnt/β-catenin pathway with increased expression of Wnt3, Lrp5 and β-catenin and to promote the accumulation of active β-catenin in the nucleus to support proliferation. Moreover, this stimulation of intestinal epithelial proliferation is necessary for the process of repairing TNF damage.

Interestingly, *L. reuteri* maintained the activation of the Wnt/β-catenin pathway to guarantee the proliferation of intestinal epithelia even without R-Spondin in the culture medium. We further demonstrated that *L. reuteri* itself induced the expression of R-spondins to maintain the activation of the Wnt/β-catenin pathway. This interesting phenomenon was further verified by the increased density of EdU^+ cells in organoids. These results indicated that *Lactobacillus* is able to stimulate the proliferative ability to protect the integrity of the intestinal mucosal barrier. ISCs are the basis of intestinal epithelial proliferation, reside in small intestine crypts and are capable of supporting intestinal epithelial regeneration.[48,49] Recent studies suggested that quiescent $Bmi1^+$ ISCs play a larger role in epithelial repair than in basal homeostasis since $Bmi1^+$ ISCs contribute to injury-associated repair upon quantitative loss of the $Lgr5^+$ population or crypt injury.[50,51] We also found that the mRNA expression levels of ISC molecular markers, such as Lgr5, Olfm4 and Ascl2, were increased by *L. reuteri* D8. Moreover, *L. reuteri* stimulated the protein expression of Lgr5 to support proliferation, which was also consistent with enhanced $Lgr5^+$ cell numbers in crypts. *L. reuteri* D8 could also increase Bmi1 expression compared to that induced by TNF damage, which indicated that *L. reuteri* D8 could activate $Bmi1^+$ ISCs to accelerate the repair process.

C. rodentium is a natural mouse pathogen related to *E. coli* that also serves as a model of infection that is mainly restricted to the intestinal lumen.[52,53] Here, we used *C. rodentium* to induce intestinal inflammation and found that the pathogen induced significant intestinal damage, including reduced body weight. However, *L. reuteri* D8 could colonize in the intestine and alleviated this symptom caused by *C. rodentium*, which may have been attributed to the colonization of *L. reuteri* and inhibition of *C. rodentium* colonization. Furthermore, *L. reuteri* exhibited no obvious effect on intestinal morphology under physiological conditions and showed an ability to repair damaged intestinal epithelia induced by *C. rodentium* treatment. The reduced pathological scores and LPS concentrations in serum indicated that *L. reuteri* protected the integrity and function of the intestinal mucosa, which is also related to reducing TNF and IL-1β secretion.

Furthermore, *L. reuteri* D8 also ameliorated *C. rodentium*-induced crypt hyperplasia by moderately activating the Wnt/β-catenin pathway to avoid overactivation. The gentle regulation and protective effect of *L. reuteri* was also proven with suitable c-Myc expression and PCNA and Lgr5 densities. In addition to controlling proliferation, *L. reuteri* also induced ISC differentiation toward Paneth cells. Paneth cells are essential for the proliferation of ISCs via the secretion of EGF, TGF, Wnt3 and the Notch ligand Dll4, signals that are all essential for stem cell maintenance in culture.[54] *L. reuteri* D8 also maintained the number of Paneth cells and lysozyme expression at normal levels in organoids after damage induced by TNF. These results implied that *Lactobacillus* can maintain ISC niches related to Paneth cells and explained the accelerated proliferation to initiate the repair. The Defa1 and Defa6 genes encode defensins, while Lyz-1 encodes lysozyme, which are all antimicrobial peptides secreted by Paneth cells to inhibit bacterial invasion.[55] The increased mRNA expression levels of antimicrobial peptide genes, such as Defa1, Defa6 and Lyz-1, in mice are helpful to prevent *C. rodentium* infection, which may explain the reduced colonization of *C. rodentium* in feces. However, the stimulatory effect of *L. reuteri* on intestinal epithelium proliferation and differentiation toward Paneth cells disappeared with the application of the Wnt antagonist Wnt-C59 both in vivo and in vitro.

In conclusion, we demonstrate that *L. reuteri* has the ability to increase the expression of

R-spondins and then to activate the Wnt/β-catenin pathway at a moderate level to stimulate the proliferation of intestinal epithelia and repair the epithelial damage caused by TNF in intestinal organoids or *C. rodentium* infection in mice. Moreover, *L. reuteri* also increased the number of Paneth cells and the expression of antimicrobial peptides, such as Defa1, Defa6 and Lyz-1, to inhibit *C. rodentium* colonization. This study indicated that intestinal microbiota, such as *Lactobacillus*, could modulate ISC proliferation and differentiation to protect the intestinal mucosal barrier against intestinal inflammation.

Materials and methods

Animals and bacterial strains

C57BL/6 mice (4 weeks old, specific pathogen-free) were purchased from the Animal Research Center of Yangzhou University. All animal studies were approved by the Institutional Animal Care and Use Committee of Nanjing Agricultural University. The *L. reuteri* strain was confirmed by 16 S rDNA sequencing results (GenBank MF850249) and grown in MRS agar medium at 37°C. The *C. rodentium* strain ATCC51459 was kindly provided by Professor Chundong Yu at Xiamen University and grown in Luria Broth (LB) at 37°C.

Mouse experiments

Four-week-old C57BL/6 mice were orally administered live or heat-killed *L. reuteri* D8 (10^8 CFU) for 28 days according to the detailed methods listed in Figures 5(a) and 7(a). Intestinal inflammation was induced by administration of *C. rodentium* on the 14th day. A Wnt signaling pathway antagonist (Selleck, USA), Wnt-C59 (5 mg/kg), was orally administered beginning on the 12th day and continued for the remaining days daily. The mice were sacrificed after subjection to the different treatments on the 28th day. Intestinal tissues were fixed with 4% paraformaldehyde, embedded in paraffin wax, sliced, and stained with hematoxylin and eosin. The crypt depth of the ileum and histological pathology were detected under light microscopy. The pathological scoring method was carried out as previously described.[6]

Intestinal organoid isolation and culture

Intestinal organoids were isolated and cultured as described previously with the modifications indicated.[15] Briefly, the small intestines of 4-week-old C57BL/6 wild-type mice were opened longitudinally, and villi were scraped off using a coverslip. The intestine was cut into 1–2 cm pieces and washed several times with cold phosphate buffered saline (PBS). The pieces were then incubated with 2 mM ethylenediaminetetraacetic acid (EDTA) in PBS for 30 min at 4°C on a rotating wheel, and crypts were detached from the basal membrane by vigorous shaking. Crypts enriched in the supernatant were passed through a 70 μm strainer and centrifuged at 800 g. The pelleted crypts were resuspended and seeded in Matrigel (BD Bioscience) on a prewarmed 24-well plate and incubated for 15 min at 37°C. Then, 500 μl of complete crypt culture medium, which contained advanced DMEM/F12 supplemented with 2 mM GlutaMax (Life Technologies), 10 mM HEPES, 100 μg/mL penicillin/streptomycin, N2 supplement (Life Technologies), B27 supplement (Life Technologies), epidermal growth factors [50 ng/mL EGF (Peprotech), 100 ng/mL Noggin (Peprotech), 500 ng/mL R-spondin (Peprotech), and 10 μM Y-27632 (Selleck)], was added. Intestinal organoids were cultured at 37°C in a 5% CO_2 atmosphere.

Intestinal organoid treatment, observation and measurement

Under physiological conditions, intestinal organoids were first co-cultured with *L. reuteri* D8 (10^6 CFU) in Matrigel for 48 h. To detect the effect of *L. reuteri* D8 on nuclear accumulation of active β-catenin, intestinal organoids were co-cultured with *L. reuteri* D8 (10^6 CFU) or Wnt agonist 1(10 μM, Selleck) for 24 h. To detect the repair effect of *L. reuteri*, intestinal organoids were pretreated with live *L. reuteri* D8 (10^6 CFU) or the Wnt antagonist Wnt-C59 (100 nM) for 24 h and then treated with TNF (60 ng/ml) for 12 h or *C. rodentium* (10^6 CFU) for 24 h to induce intestinal damage to the organoids. Then, *L. reuteri* D8 (10^6 CFU) was cocultured with the organoids for an additional 24 h. To test whether *L. reuteri* D8 can replace R-spondin to activate the Wnt/β-catenin signaling pathway, intestinal organoids were cocultured with *L. reuteri* D8 or heat-

killed (HK)-*L. reuteri* D8 (10^6 CFU) in the absence of R-spondin-1 for 48 h.

The surface area of intestinal organoids was measured according to a previous study.[31] Briefly, if all organoids in a well could not be measured, several random nonoverlapping pictures were acquired from each well using a Zeiss 710 laser scanning confocal microscope. Organoids touching the edge of the images were excluded from the counting. Organoid perimeters for area measurements were defined manually and by automated determination using the Analyze Particle function of ImageJ software (National Institutes of Health, USA). The sizes of the largest and smallest organoids in the reference well were measured manually, and their areas were used as the reference values for setting the minimal and maximal particle sizes.

Detection of epithelial proliferation and apoptosis in intestinal organoids

Intestinal organoids in each well were incubated with 100 μL of 50 μM EdU medium for 2 h, and the culture medium was then discarded. The organoids were fixed with paraformaldehyde for 1 h at 4°C and permeabilized with 0.4% Triton X-100 for 30 min; Hoechst 33342 was used to stain nuclei. Organoids were then detected with a confocal microscope, and the mean density of EdU^+ cells was analyzed by Image-Pro Plus software.

Apoptotic cells were detected with Annexin V and propidium iodide (PI) staining assays (Multi Science) according to the manufacturer's protocol. Briefly, organoids were digested with accutase (Millipore) for 25 min at 37°C, and single-cell suspensions were obtained. The cells were harvested and washed with PBS, incubated with 5 μL of Annexin V-FITC and 5 μL of PI-FL3 for 10 min and detected with a FACS Calibur flow cytometer (BD Company). Single cells were gated using FSC and SSC parameters, and apoptotic organoid cells were analyzed at FL-1 and FL-3 by FACS.

RT-qPCR

Total RNA was extracted from mouse intestinal organoids or tissues by RNAiso Plus (Takara). RNA was reverse transcribed with a PrimeScript RT Reagent Kit (Takara) and customized primers designed to amplify fragments of the target genes with SYBR master mix (Takara) using the QuantStudio 7 Flex System (Applied Biosystems). Relative amounts of mRNA were calculated using the $2^{-\Delta\Delta}$ CT method, and GAPDH served as the housekeeping gene. Fold change values were calculated for genes expressed in experimental vs control conditions. The primers used in this study are listed in Table 1.

Western blot analysis

Intestinal organoids were lysed in radioimmunoprecipitation assay (RIPA) buffer (50 mM Tris-HCl (pH 7.4), 1% NP-40, 150 mM NaCl) containing a protease inhibitor cocktail (Thermo Scientific). The BCA protein quantification kit (Thermo Scientific) was used to determine protein concentrations. Equal amounts of protein were separated by SDS-PAGE and then electrotransferred onto polyvinylidene fluoride (PVDF) membranes (Millipore). The following antibodies were used: rabbit anti-Lgr5 (Abcam, 1:1000), rabbit anti-lysozyme (Abcam, 1:10000), rabbit anti-β-catenin (Abcam, 1:1000), rabbit anti-active-β-catenin (Cell Signaling Technology 1:1000), mouse anti-tubulin (Sigma, 1:1000), goat anti-rabbit secondary antibodies (Vazyme, 1:5000) and mouse anti-rabbit secondary antibodies (Vazyme, 1:5000). Signals were detected using enhanced chemiluminescence (ECL) kits and a chemiluminescence/fluorescence image analysis system (Tanon).

Immunofluorescence assay

Two-centimeter sections of ileum were collected from each mouse in the different groups, fixed overnight in 4% paraformaldehyde, and then embedded in optimal cutting temperature (OCT) compound. The ileum was sectioned at 5 μm, rinsed in PBS, permeabilized with 0.4% Triton X-100 for 30 min, washed five times with PBS and incubated for 2 h in 5% bovine serum albumin (BSA) to reduce nonspecific background. For PCNA staining, ileum sections were permeabilized and incubated with an anti-mouse PCNA antibody (1:100, Abcam) overnight. For Paneth cell and ISC staining, tissue sections or intestinal organoids were fixed with paraformaldehyde for 1 h, permeabilized with 0.4% Triton X-100 for 30 min and incubated in 5% BSA for 2 h. The tissues or organoids

Table 1. Primer sequences used for RT-qPCR.

Target gene	Primer sense (5′-3′)	Primer antisense (5′-3′)
mWnt3	CTCGCTGGCTACCCAATTTG	CTTCACACCTTCTGCTACGCT
mLrp5	CTGCATAGCATTGAACGGGC	GGTCCAGCGTGTAGTGTGAA
mc-Myc	GCTCGCCCAAATCCTGTACCT	TCTCCACAGACACCACATCAATTTC
mcyclin	CATGTATCATCTAGCCATGCACGAG	ATGCACAACAGGCCGCTACA
mKi67	ACCGTGGAGTAGTTTATCTGGG	TGTTTCCAGTCCGCTTACTTCT
mLgr5	CTGAGACAGGTTCCGGAGGA	GAGATGCAGAACCACGAGGC
mAscl2	AAGCACACCTTGACTGGTACG	AAGTGGACGTTTGCACCTTCA
mOlfm4	CAGCCACTTTCCAATTTCACTG	GCTGGACATACTCCTTCACCTTA
mBmi1	TTCATTGTCTTTTCCGCCCG	AGTACCCTCCACACAGGACA
mMsi1	CCTCTCACGGCTTATGGGC	CTGTGGCAATCAAGGGACC
mLyz1	GCCAAGGTCTACAATCGTTGTGAGTTG	CAGTCAGCCAGCTTGACACCACG
mDefa6	CCTTCCAGGTCCAGGCTGAT	TGAGAAGTGGTCATCAGGCAC
mDefa1	TCAAGAGGCTGCAAAGGAAGAGAAC	TGGTCTCCATGTTCAGCGACAGC
m IL-1β	CCTTCCAGGATGAGGACATGA	TGAGTCACAGAGGATGGGCTC
mTNF	TACTGAACTTCGGGGTGATTGGTCC	CAGCCTTGTCCCTTGAAGAGAACC
r-spondin1	TGTGAAATGAGCGAGTGGTCC	TCTCCCAGATGCTCCAGTTCT
r-spondin2	TTGCATAGAGGCCGCTGCTTT	CTGGTCAGAGGATCAGGAATG
r-spondin3	GTACACTGTGAGGCCAGTGAA	ATGGCTAGAACACCTGTCCTG
mGAPDH	ATGGTGAAGGTCGGTGTGAA	TGGAAGATGGTGATGGGCTT

were then incubated with primary antibodies (anti-rabbit lysozyme antibody, 1:200, Abcam; anti-rabbit Lgr5 antibody, 1:200, Affinity; anti-active-β-catenin, 1:200, Cell Signaling Technology) overnight at 4°C. The samples were incubated with a goat anti-rabbit antibody conjugated to Alexa Fluor 594 (1:250, Abcam) or Alexa Fluor 488 (1:250, Abcam) for 60 min at room temperature. Nuclei were stained with Hoechst 33342 (1:5000, Invitrogen) for 5 min. The samples were examined with a Zeiss 710 laser scanning confocal microscope. Fluorescence images were collected for further qualitative and quantitative analyzes. The numbers of lysozyme$^+$ and Lgr5$^+$ cells per crypt were counted in organoids. Analysis of PCNA, Lgr5, and lysozyme$^+$ cells in the ileum was performed similarly to the method used to analyze the optical density of EdU$^+$ cells.

L. reuteri D8 colonization

To verify colonization of *L. reuteri* D8 in the intestine, mice were orally administered 10^8 CFU *L. reuteri* D8 suspended in 200 μL of PBS only once. Fresh mouse feces was collected at the indicated time points (0, 4, 8, 16, 24, 48, 72, 96 and 168 h) and added to 2 ml of PBS before being cultured on MRS plates containing 500 μg/ml tetracycline at 37°C for 16 h to count the bacterial colonies. Moreover, D8 was stained with BacLight™ Bacterial Green Stain (B-35000, Molecular Probes) according to the manufacturer's instructions. In brief, 10^8 CFU *L. reuteri* D8 and a 100 μM working solution of BacLight bacterial stain dissolved in dimethyl sulfoxide (DMSO) were mixed and incubated for 15 min at room temperature. The D8 samples were washed with PBS to remove excess dye. Mice were administered 200 μL of PBS or 10^8 CFU *L. reuteri* D8 labeled with BacLight™ Bacterial Green Stain only once to detect bacterial colonization. After 16 h, a 2-cm section of ileum was collected from the mouse, frozen immediately with liquid nitrogen, embedded in OCT, sectioned at 5 μm and rinsed in PBS. Then, the sample was examined with a Zeiss 710 laser scanning confocal microscope.

Quantitation of C. rodentium burden

To assess the clearance of *C. rodentium*, fecal pellets were collected from each mouse on the 5th and 10th days post infection. The fecal pellets were weighed, homogenized, serially diluted, and plated on selective MacConkey agar plates. Bacterial colonies were enumerated after overnight incubation. *C. rodentium* colonies were easily distinguished by appearance, and the MacConkey agar-plated bacterial culture strain DBS100 was used as a positive control. Bacterial counts are reported as CFU per gram.

Cytokines and LPS detection

Small intestines were collected from euthanized mice and then homogenized and centrifuged. The

supernatants were stored at −20°C until use for cytokine analysis. Cytokine analysis was performed on thawed samples with IL-1β and TNF ELISA kits (SenBeiJia Bio Tech) according to the manufacturer's protocol. To calibrate the concentrations of TNF and IL-1β in the supernatants, a BCA protein quantification kit (Thermo Scientific) was used to determine the protein concentrations in the supernatants. For the detection of serum LPS, blood samples were collected from mice in each group. Serum was collected after centrifugation and stored at −70°C until detection with an LPS kit (Yifeixue Bio Tech).

Statistical analysis

The results are expressed as the means ± SDs. One-way ANOVA was employed to determine significant differences among multiple groups, and the t-test was employed to assess differences between two groups. $^{*}P < .05$ and $^{**}P < .01$. Data were combined from at least three independent experiments unless otherwise stated.

Author Contributions

Haiqin Wu, Shuang Xie and Zhihua Wang were responsible for performing the experiments and data analysis and for writing the manuscript.

Yuchen Li established the coculture system of organoids and LPLs.

Haiqin Wu, Minjuan Wang and Jinfeng Miao were responsible for the animal experiments.

Qinghua Yu was responsible for the conception and design of the study, data collection, drafting of the article, and final approval of the version submitted.

Acknowledgments

We appreciate Jerrold R Turner of the University of Chicago for providing support regarding intestinal organoid technology.

Disclosure of Potential Conflicts of Interest

No potential conflicts of interest were disclosed.

Funding

This study was supported by the National Key R&D Program of China [2018YFE0127300]; the National Natural Science Foundation of China [31972631, 31502024 and 31930109]; the State Key Laboratory of Veterinary Etiological Biology, Lanzhou Veterinary Research Institute, Chinese Academy of Agricultural Sciences [SKLVEB2019KFKT004]; the Fundamental Research Funds for the Central Universities [JCQY201906 and Y0201700175]; and a project funded by the Priority Academic Program Development of Jiangsu Higher Education Institutions [PAPD].

References

1. Citi S. Intestinal barriers protect against disease. Science. 2018;359:1097–1098. doi:10.1126/science.aat0835.
2. Bjarnason I, Scarpignato C, Holmgren E, Olszewski M, Rainsford KD, Lanas A. Mechanisms of damage to the gastrointestinal tract from nonsteroidal anti-inflammatory drugs. Gastroenterology. 2018;154:500–514. doi:10.1053/j.gastro.2017.10.049.
3. Sommer F, Anderson JM, Bharti R, Raes J, Rosenstiel P. The resilience of the intestinal microbiota influences health and disease. Nat Rev Microbiol. 2017;15:630–638. doi:10.1038/nrmicro.2017.58.
4. Luissint AC, Parkos CA, Nusrat A. Inflammation and the intestinal barrier: leukocyte-epithelial cell interactions, cell junction remodeling, and mucosal repair. Gastroenterology. 2016;151:616–632. doi:10.1053/j.gastro.2016.07.008.
5. Yue Y, Wu SC, Li ZK, Li J, Li XF, Xiang J, Ding H. Wild jujube polysaccharides protect against experimental inflammatory bowel disease by enabling enhanced intestinal barrier function. Food Funct. 2015;6:2568–2577. doi:10.1039/C5FO00378D.
6. Odenwald MA, Turner JR. The intestinal epithelial barrier: a therapeutic target? Nat Rev Gastro Hepat. 2017;14:9–21. doi:10.1038/nrgastro.2016.169.
7. Martens EC, Neumann M, Desai MS. Interactions of commensal and pathogenic microorganisms with the intestinal mucosal barrier. Nat Rev Microbiol. 2018;16:457–470. doi:10.1038/s41579-018-0036-x.
8. Dickson I. Gut microbiota: oral bacteria: a cause of IBD? Nat Rev Gastroenterol Hepatol. 2018;15:4–5.
9. Imhann F, Vich Vila A, Bonder MJ, Fu J, Gevers D, Visschedijk MC, Spekhorst LM, Alberts R, Franke L, van Dullemen HM, et al. Interplay of host genetics and gut microbiota underlying the onset and clinical presentation of inflammatory bowel disease. Gut. 2018;67:108–119. doi:10.1136/gutjnl-2016-312135.
10. Sanchez B, Delgado S, Blanco-Miguez A, Lourenco A, Gueimonde M, Margolles A. Probiotics, gut microbiota, and their influence on host health and disease. Mol Nutr Food Res. 2017;61:1600240.
11. Indian Council of Medical Research Task F, Co-ordinating Unit I, Co-ordinating Unit DBT. ICMR-DBT guidelines for evaluation of probiotics in food. Indian J Med Res. 2011;134:22–25.
12. Probiotics in food : health and nutritional properties and guidelines for evaluation : Report of a Joint FAO/WHO Expert Consultation on Evaluation of Health

and Nutritional Properties of Probiotics in Food including Powder Milk with Live Lactic Acid Bacteria, Cordoba, Argentina, 1-4 October 2001 [and] Report of a Joint FAO/WHO Working Group on Drafting Guidelines for the Evaluation of Probiotics in Food, London, Ontario, Canada, 30 April -1 May 2002. Rome [Italy]: Food and Agriculture Organization of the United Nations, World Health Organization, 2006.
13. Yen TH, Wright NA. The gastrointestinal tract stem cell niche. Stem Cell Rev. 2006;2:203–212. doi:10.1007/s12015-006-0048-1.
14. Barker N, Huch M, Kujala P, van de Wetering M, Snippert HJ, van Es JH, Sato T, Stange DE, Begthel H, van den Born M, et al. Lgr5(+ve) stem cells drive self-renewal in the stomach and build long-lived gastric units in vitro. Cell Stem Cell. 2010;6:25–36. doi:10.1016/j.stem.2009.11.013.
15. Sato T, Vries RG, Snippert HJ, van de Wetering M, Barker N, Stange DE, van Es JH, Abo A, Kujala P, Peters PJ, et al. Single Lgr5 stem cells build crypt-villus structures in vitro without a mesenchymal niche. Nature. 2009;459:262–265. doi:10.1038/nature07935.
16. Espada J, Calvo MB, Diaz-Prado S, Medina V. Wnt signalling and cancer stem cells. Clin Transl Oncol. 2009;11:411–427. doi:10.1007/s12094-009-0380-4.
17. Van Parys A, Boyen F, Leyman B, Verbrugghe E, Maes D, Haesebrouck F, Pasmans F. Induction of seroconversion and persistence of Salmonella Typhimurium in pigs are strain dependent. Comp Immunol Microb. 2013;36:465–471. doi:10.1016/j.cimid.2013.03.007.
18. Monteiro C, Papenfort K, Hentrich K, Ahmad I, Le Guyon S, Reimann R, Grantcharova N, Römling U. Hfq and Hfq-dependent small RNAs are major contributors to multicellular development in Salmonella enterica serovar typhimurium. RNA Biol. 2012;9:489–502. doi:10.4161/rna.19682.
19. Rao RK, Samak G. Protection and Restitution of gut barrier by probiotics: nutritional and clinical implications. Curr Nutr Food Sci. 2013;9:99–107. doi:10.2174/1573401311309020004.
20. Lightfoot YL, Selle K, Yang T, Goh YJ, Sahay B, Zadeh M, Owen JL, Colliou N, Li E, Johannssen T, et al. SIGNR3-dependent immune regulation by Lactobacillus acidophilus surface layer protein A in colitis. Embo J. 2015;34:881–895. doi:10.15252/embj.201490296.
21. Jones RM, Luo L, Ardita CS, Richardson AN, Kwon YMMercante JW. Symbiotic lactobacilli stimulate gut epithelial proliferation via nox-mediated generation of reactive oxygen species. Embo J. 2013;32:3017–28.
22. Campana R, Federici S, Ciandrini E, Baffone W. Antagonistic activity of lactobacillus acidophilus ATCC 4356 on the growth and adhesion/invasion characteristics of human campylobacter jejuni. Curr Microbiol. 2012;64:371–378. doi:10.1007/s00284-012-0080-0.
23. Liu HY, Roos S, Jonsson H, Ahl D, Dicksved J, Lindberg JE, Lundh T. Effects of Lactobacillus johnsonii and Lactobacillus reuteri on gut barrier function and heat shock proteins in intestinal porcine epithelial cells. Physiol Rep. 2015;3:e12355. doi:10.14814/phy2.12355.
24. Yu Q, Yuan L, Deng J, Yang Q. Lactobacillus protects the integrity of intestinal epithelial barrier damaged by pathogenic bacteria. Front Cell Infect Microbiol. 2015;5:26. doi:10.3389/fcimb.2015.00026.
25. Mahe MM, Aihara E, Schumacher MA, Zavros Y, Montrose MH, Helmrath MA, Sato T, Shroyer NF. Establishment of gastrointestinal epithelial organoids. Curr Protoc Mouse Biol. 2013;3:217–240. doi:10.1002/9780470942390.2013.3.issue-4.
26. Hou Q, Ye L, Huang L, Yu Q. The research progress on intestinal stem cells and its relationship with intestinal microbiota. Front Immunol. 2017;8:599. doi:10.3389/fimmu.2017.00599.
27. Peck BCE, Shanahan MT, Singh AP, Sethupathy P. Gut microbial influences on the mammalian intestinal stem cell niche. Stem Cells Int. 2017;2017:5604727. doi:10.1155/2017/5604727.
28. Pinto D, Gregorieff A, Begthel H, Clevers H. Canonical Wnt signals are essential for homeostasis of the intestinal epithelium. Genes Dev. 2003;17:1709–1713. doi:10.1101/gad.267103.
29. Lebensohn AM, Rohatgi R. R-spondins can potentiate WNT signaling without LGRs. Elife. 2018;7. doi:10.7554/eLife.33126.
30. Kim KA, Wagle M, Tran K, Zhan XM, Dixon MA, Liu SC, Gros D, Korver W, Yonkovich S, Tomasevic N, et al. R-Spondin family members regulate the Wnt pathway by a common mechanism. Mol Biol Cell. 2008;19:2588–2596. doi:10.1091/mbc.e08-02-0187.
31. Hou QH, Ye LL, Liu HF, Huang LL, Yang Q, Turner JR, Yu Q. Lactobacillus accelerates ISCs regeneration to protect the integrity of intestinal mucosa through activation of STAT3 signaling pathway induced by LPLs secretion of IL-22. Cell Death Differ. 2018;25:1657–1670. doi:10.1038/s41418-018-0070-2.
32. Salic A, Mitchison TJ. A chemical method for fast and sensitive detection of DNA synthesis in vivo. Proc Natl Acad Sci USA. 2008;105:2415–2420. doi:10.1073/pnas.0712168105.
33. Wang D, Peregrina K, Dhima E, Lin EY, Mariadason JM, Augenlicht LH. Paneth cell marker expression in intestinal villi and colon crypts characterizes dietary induced risk for mouse sporadic intestinal cancer. Proc Natl Acad Sci USA. 2011;108:10272–10277. doi:10.1073/pnas.1017668108.
34. Roth S, Franken P, Sacchetti A, Kremer A, Anderson K, Sansom O, Fodde R. Paneth cells in intestinal homeostasis and tissue injury. PLoS One. 2012;7:e38965. doi:10.1371/journal.pone.0038965.
35. Bonfini A, Liu X, Buchon N. From pathogens to microbiota: how Drosophila intestinal stem cells react to gut microbes. Dev Comp Immunol. 2016;64:22–38. doi:10.1016/j.dci.2016.02.008.

36. Ayyaz A, Jasper H. Intestinal inflammation and stem cell homeostasis in aging Drosophila melanogaster. Front Cell Infect Mi. 2013;3:98.
37. Zhang YJ, Li S, Gan RY, Zhou T, Xu DP, Li HB. Impacts of gut bacteria on human health and diseases. Int J Mol Sci. 2015;16:7493–7519. doi:10.3390/ijms16047493.
38. Chatfield SN, Dorman CJ, Hayward C, Dougan G. Role of ompr-dependent genes in salmonella-typhimurium virulence - mutants deficient in both ompc and ompf are attenuated invivo. Infect Immun. 1991;59:449–452. doi:10.1128/IAI.59.1.449-452.1991.
39. Huang Y, Wang JF, Quan GH, Wang XJ, Yang LF, Zhong LL. Lactobacillus acidophilus ATCC 4356 prevents atherosclerosis via inhibition of intestinal cholesterol absorption in apolipoprotein E-Knockout mice. Appl Environ Microb. 2014;80:7496–7504. doi:10.1128/AEM.02926-14.
40. Metcalfe C, Kljavin NM, Ybarra R, de Sauvage FJ. Lgr5+ stem cells are indispensable for radiation-induced intestinal regeneration. Cell Stem Cell. 2014;14:149–159. doi:10.1016/j.stem.2013.11.008.
41. Tracey KJ, Fong Y, Hesse DG, Manogue KR, Lee AT, Kuo GC, Lowry SF, Cerami A. Anti-cachectin Tnf monoclonal-antibodies prevent septic shock during lethal bacteremia. Nature. 1987;330:662–664. doi:10.1038/330662a0.
42. Piguet PF, Vesin C, Guo J, Donati Y, Barazzone C. TNF-induced enterocyte apoptosis in mice is mediated by the TNF receptor 1 and does not require p53. Eur J Immunol. 1998;28:3499–3505. doi:10.1002/()1521-4141.
43. Taylor CT, Dzus AL, Colgan SP. Autocrine regulation of epithelial permeability by hypoxia: role for polarized release of tumor necrosis factor alpha. Gastroenterology. 1998;114:657–668. doi:10.1016/S0016-5085(98)70579-7.
44. Farin HF, Van Es JH, Clevers H. Redundant sources of Wnt regulate intestinal stem cells and promote formation of Paneth cells. Gastroenterology. 2012;143:1518–29 e7. doi:10.1053/j.gastro.2012.08.031.
45. Clevers H, Loh KM, Nusse R. Stem cell signaling. An integral program for tissue renewal and regeneration: Wnt signaling and stem cell control. Science. 2014;346:1248012. doi:10.1126/science.1248012.
46. Hao HX, Xie Y, Zhang Y, Charlat O, Oster E, Avello M, Lei H, Mickanin C, Liu D, Ruffner H, et al. ZNRF3 promotes Wnt receptor turnover in an R-spondin-sensitive manner. Nature. 2012;485:195–200. doi:10.1038/nature11019.
47. Koo BK, Spit M, Jordens I, Low TY, Stange DE, van de Wetering M, van Es JH, Mohammed S, Heck AJR, Maurice MM, et al. Tumour suppressor RNF43 is a stem-cell E3 ligase that induces endocytosis of Wnt receptors. Nature. 2012;488:665–669. doi:10.1038/nature11308.
48. Barker N, van Es JH, Kuipers J, Kujala P, van den Born M, Cozijnsen M, Haegebarth A, Korving J, Begthel H, Peters PJ, et al. Identification of stem cells in small intestine and colon by marker gene Lgr5. Nature. 2007;449:1003–1007. doi:10.1038/nature06196.
49. Sangiorgi E, Capecchi MR. Bmi1 is expressed in vivo in intestinal stem cells. Nat Genet. 2008;40:915–920. doi:10.1038/ng.165.
50. Yan KS, Chia LA, Li X, Ootani A, Su J, Lee JY, Su N, Luo Y, Heilshorn SC, Amieva MR, et al. The intestinal stem cell markers Bmi1 and Lgr5 identify two functionally distinct populations. Proc Natl Acad Sci USA. 2012;109:466–471. doi:10.1073/pnas.1118857109.
51. Costa BP, Goncalves AC, Abrantes AM, Alves R, Matafome P, Seica R, Sarmento-Ribeiro AB, Botelho MF, Castro-Sousa F. Intestinal epithelial stem cells: distinct behavior after surgical injury and teduglutide administration. J Invest Surg. 2017;31:1–10.
52. Jain U, Cao Q, Thomas NA, Woodruff TM, Schwaeble WJ, Stover CM, Stadnyk AW. Properdin provides protection from Citrobacter rodentium-induced intestinal inflammation in a C5a/IL-6-dependent manner. J Immunol. 2015;194:3414–3421. doi:10.4049/jimmunol.1401814.
53. Luperchio SA, Schauer DB. Molecular pathogenesis of Citrobacter rodentium and transmissible murine colonic hyperplasia. Microbes Infect. 2001;3:333–340. doi:10.1016/S1286-4579(01)01387-9.
54. Sato T, van Es JH, Snippert HJ, Stange DE, Vries RG, van den Born M, Barker N, Shroyer NF, van de Wetering M, Clevers H, et al. Paneth cells constitute the niche for Lgr5 stem cells in intestinal crypts. Nature. 2011;469:415–418. doi:10.1038/nature09637.
55. Arijs I, De Hertogh G, Lemaire K, Quintens R, Van Lommel L, Van Steen K, Leemans P, Cleynen I, Van Assche G, Vermeire S, et al. Mucosal gene expression of antimicrobial peptides in inflammatory bowel disease before and after first infliximab treatment. PLoS One. 2009;4:e7984. doi:10.1371/journal.pone.0007984.